Differential Interaction of Tubulin Isotypes with the Antimitotic Compound IKP-104†

Israr A. Khan,*,‡ Isao Tomita,§ Fukutaro Mizuhashi,|| and Richard F. Ludueña‡

Department of Biochemistry, University of Texas Health Science Center, San Antonio, Texas 78284, Shizuoka Sangyo University, Shizuoka, Japan, and Kumiai Chemical Industry Company Ltd., Tokyo, Japan

Received February 11, 2000; Revised Manuscript Received May 31, 2000

ABSTRACT: The tubulin molecule is a heterodimer composed of two polypeptide chains, designated α and *β*; both α and *β* exist in numerous isotypic forms, which differ in their assembly and drug binding properties. 2-(4-Fluorophenyl)-1-(2-chloro-3,5-dimethoxyphenyl)-3-methyl-6-phenyl-4(1*H*)-pyridinone (IKP-104) is an antimitotic compound which inhibits polymerization and induces depolymerization of microtubules [Mizuhashi, F., et al. (1992) *Jpn. J. Cancer Res. 83,* 211]. Since the previous work was undertaken with isotypically unfractionated tubulin, we have investigated the interactions of IKP-104 with the isotypically purified tubulin dimers ($\alpha\beta_{II}$, $\alpha\beta_{III}$, and $\alpha\beta_{IV}$). We find that IKP-104 binds to $\alpha\beta_{II}$ and $\alpha\beta_{III}$ at two classes of binding sites. However, affinities for each class of site are much weaker for $\alpha\beta_{III}$ than for $\alpha\beta_{II}$. Interestingly, the low-affinity site on $\alpha\beta_{IV}$ was not detectable. Its high-affinity site was weaker than those of either $\alpha\beta_{II}$ or $\alpha\beta_{III}$. In a pattern consistent with these results, IKP-104 inhibited assembly better with $\alpha\beta_{II}$ than with the other two dimers. Higher concentrations of IKP-104 induced formation of spiral aggregates from $\alpha\beta_{II}$ and $\alpha\beta_{III}$ but not from $\alpha\beta_{IV}$. Our results suggest that the interaction of IKP-104 with tubulin isotypes is very complex: $\alpha\beta_{II}$ and $\alpha\beta_{III}$ differ quantitatively in their interaction with IKP-104, and $\alpha\beta_{IV}$'s interaction differs both quantitatively and qualitatively from those of the other two dimers.

IKP-104[1] is an antitumor compound which inhibits growth of murine as well as human tumor cell lines and a murine solid tumor in vitro (*1*). Although the mechanism of action of IKP-104 is not known, the compound has been shown to inhibit polymerization and induce depolymerization of microtubules in vivo and in vitro (*2*−*4*). Tubulin, which is the major constituent protein of microtubules (*5*), undergoes a large conformational change upon interacting with IKP-104 (*3*, *4*, *6*−*9*). IKP-104 has been thought to interact with tubulin in a region (*3*) where the *Vinca* alkaloids interact (*10*). It has been shown previously that there are two classes of binding sites on tubulin for IKP-104: one high-affinity site and one low-affinity site (*4*). The high-affinity site stabilizes the tubulin molecule against decay, whereas the low-affinity site, once occupied by IKP-104, accelerates the decay or apparent unfolding of the tubulin molecule which is manifested in increased exposure of sulfhydryl groups and hydrophobic areas on tubulin (*8*).

Both α- and *β*-subunits of tubulin exist as multiple isotypes, each encoded by a different gene (*11*). In mammals, there are six α- and seven *β*-isotypes (*12*). The differences among the *β*-isotypes, which are found mostly within the C-terminal region, have been highly conserved throughout evolution. Tubulin dimers isotypically purified by their *β*-subunits differ from each other in their assembly, dynamics, cellular distribution, post-translational modification, and conformation (*13*−*20*). Some of the most interesting differences among the isotypes involve their interactions with ligands. The $\alpha\beta_{III}$ dimer interacts much less strongly with colchicine, vinblastine, and paclitaxel than do the $\alpha\beta_{II}$ and $\alpha\beta_{IV}$ dimers (*21*−*24*). Because IKP-104 appears to have such a complex and unique set of interactions with tubulin, it was of interest to investigate its individual interactions with isotypically purified tubulin dimers. We therefore examined the binding of IKP-104 to the isotypically purified dimers $\alpha\beta_{II}$, $\alpha\beta_{III}$, and $\alpha\beta_{IV}$ as well as its effect on their polymerization. We found that, as with unfractionated tubulin, both $\alpha\beta_{II}$ and $\alpha\beta_{III}$ have two classes of binding sites, differing in affinity, and that for $\alpha\beta_{III}$, each binding site has a lower affinity than does the corresponding site on $\alpha\beta_{II}$. Most surprising, however, was the observation that $\alpha\beta_{IV}$ has no detectable low-affinity binding site and that its high-affinity site had a lower affinity than the corresponding site in both $\alpha\beta_{II}$ and $\alpha\beta_{III}$. Consistent with these observations, IKP-104, at low concentrations, inhibited formation of microtubules from all three dimers but, at higher concentrations, induced

† Supported by Grants CA26376 and HL07446 from the National Institutes of Health and AQ-0726 from the Welch Foundation.

* To whom correspondence should be addressed: Department of Biochemistry, Mail Code 7760, University of Texas Health Science Center, 7703 Floyd Curl Dr., San Antonio, TX 78229-3900. Phone: (210) 567-6594. Fax: (210) 567-6595. E-mail: israr@bioc02.UTHSCSA.edu.

‡ University of Texas Health Science Center.

§ Shizuoka Sangyo University.

|| Kumiai Chemical Industry Co. Ltd.

[1] Abbreviations: IKP-104, 2-(4-fluorophenyl)-1-(2-chloro-3,5-dimethoxyphenyl)-3-methyl-6-phenyl-4(1*H*)-pyridinone; DMSO, dimethyl sulfoxide; EDTA, ethylenediaminetetraacetic acid; EGTA, ethylene glycol bis(*β*-aminoethyl ether)-*N*,*N*,*N*′,*N*′-tetraacetic acid; MES, 2-(*N*-morpholino)ethanesulfonic acid; PIPES, piperazine-*N*,*N*′-bis(2-ethanesulfonic acid); PBS, phosphate-buffered saline [0.01 M sodium phosphate (pH 7.0), 0.15 M NaCl, and 0.001 M EDTA].

10.1021/bi000331o CCC: $19.00
Published on Web 07/07/2000

formation of spiral filaments from only $\alpha\beta_{II}$ and $\alpha\beta_{III}$. Our results suggest that the effects of IKP-104 in vivo would vary greatly among tissues depending upon their tubulin isotype composition and also highlight the fact that tubulin isotypes differ from each other in their functional properties in vitro.

EXPERIMENTAL PROCEDURES

Materials. GTP was purchased from Sigma Chemicals (St. Louis, MO). IKP-104 was synthesized at the K-I Research Institute (Shizuoka, Japan). The compound was dissolved in dimethyl sulfoxide immediately before use because repeated freezing and thawing led to a dramatic loss in its ability to bind tubulin and inhibit microtubule assembly.

Purification of Tubulin Isotypes. Microtubules were prepared from bovine cerebra by the method of Fellous et al. (*25*); tubulin was purified therefrom by phosphocellulose chromatography. Microtubule-associated proteins were prepared from the microtubules and fractionated to purify tau by gel filtration as previously described (*25*). The isotypically purified $\alpha\beta_{II}$, $\alpha\beta_{III}$, and $\alpha\beta_{IV}$ tubulin dimers were prepared by immunoaffinity chromatography as described previously (*26*). All isotypically purified tubulins were stored at −80 °C until they were ready for use.

The relative amounts of $\alpha\beta_{III}$ in each tubulin sample were measured by subjecting the tubulin to SDS−PAGE on 5.5% gels (*27*). Tubulin samples were reduced and carboxymethylated prior to SDS−PAGE (*28*). Under these conditions, the β_{III} isotype has an electrophoretic mobility distinctly different from those of the β_{II} and β_{IV} isotypes, which comigrate (*29*, *30*). The immunoblotting of gels was carried out as previously described (*26*).

Tubulin Polymerization. The tubulin was thawed on ice−water and spun at 18000*g* for 6 min at 4 °C to remove any insoluble tubulin aggregates from the sample. Tubulin present in the supernatant was quantitated by the method of Lowry et al. (*31*) and mixed with IKP-104 and tau in MES buffer [0.1 M MES, 1 mM GTP, 0.5 mM $MgCl_2$, 0.1 mM EDTA, 1 mM EGTA, and 1 mM β-mercaptoethanol (pH 6.4)] at 4 °C. Unless otherwise mentioned, the final concentrations of tubulin and tau were 1.5 and 0.15 mg/mL, respectively. The temperature of the samples was raised from 4 to 37 °C, and tubulin polymerization was followed by either sedimentation or turbidimetry as described previously (*26*). All the absorbance measurements were taken using a Beckman DU7400 spectrophotometer equipped with a Peltier temperature controller.

Electron Microscopy. The mixtures of tubulin and tau were incubated for at least 30 min at 37 °C in the absence or presence of IKP-104 in MES buffer. The concentrations of tubulin and tau were 1.5 and 0.15 mg/mL, respectively. Aliquots (50 μL) were withdrawn and treated with 1% glutaraldehyde for 30 s, and then layered on 400-mesh copper grids coated with carbon over Formvar. After 1 min, the grids were washed with 4 drops of water and stained with 1% uranyl acetate for 1 min. Excess stain was removed, and after air-drying, grids were examined in a JEOL 100 CX electron microscope with an accelerating voltage of 60 kV (*26*).

IKP-104 Binding Assay. Tubulin (2 μM) and IKP-104 (0−25 μM) were mixed in 500 μL of 50 mM PIPES buffer (pH 7.0) containing 1 mM EGTA and 0.5 mM $MgCl_2$. The mixture was incubated for 30 min at 30 °C, and the fluorescence intensities of the samples were recorded in a Hitachi F-2000 spectrofluorometer. The excitation and emission wavelengths were 273 and 330 nm, respectively. The absorbance of control samples containing 0−25 μM IKP-104 (without tubulin) was also measured at 273 and 330 nm to correct the observed fluorescence intensities at 330 nm for the inner filter effect (*32*). The corrected observed fluorescence data were analyzed by using different models and equations as follows:

one-site model (high-affinity site): $F = F_1$ (1)

two-site model (high- and low-affinity sites):

$$F = F_1 + F_2 \quad (2)$$

three-site model (high-, low-, and lowest-affinity sites):

$$F = F_1 + F_2 + F_3 \quad (3)$$

$$F_1 = (F_{m1}D)/(K_{d1} + D) \quad (4)$$

$$F_2 = (F_{m2}D)/(K_{d2} + D) \quad (5)$$

$$F_3 = (F_{m3}D)/(K_{d3} + D) \quad (6)$$

where F is the total corrected observed fluorescence intensity of the tubulin and IKP-104 mixture; F_1, F_2, and F_3 are the corrected observed fluorescence intensities for the high-, low-, and lowest-affinity sites, respectively, on tubulin at any IKP-104 concentration D; F_{m1}, F_{m2}, and F_{m3} are the maximum fluorescence intensities for the high-, low-, and lowest-affinity sites on tubulin, respectively; and K_{d1}, K_{d2}, and K_{d3} are the apparent dissociation constants for the high-, low-, and lowest-affinity sites, respectively. The data were fitted using the nonlinear curve fitting software MINSQ, version 3.2 (Micromath Scientific Software, Salt Lake City, UT), as described by Chaudhuri et al. (*9*).

RESULTS

An assay for assessing the binding of IKP-104 to tubulin has been reported earlier by Chaudhuri et al. (*9*) which relies on the IKP-104-induced local conformational changes in tubulin and the increment of the fluorescence of IKP-104 in the IKP-104−tubulin complex at 451 nm (λ_{ex} = 278 nm). A nonlinear relationship exists between the increasing IKP-104 concentration and the resulting increase in IKP-104 fluorescence. However, the fidelity of this relationship appears to exist within a narrow range of IKP-104 concentrations (0−10 μM) because at higher concentrations (e.g., >10 μM IKP-104), instead of increasing, the IKP-104 fluorescence starts decreasing (results not shown). A local conformational change induced by the high concentration of the compound at its binding site on the tubulin molecule possibly perturbs the IKP-104 fluorescence. In the method presented here, we have enhanced the reliability of binding data by using a wider range of IKP-104 concentrations (0−25 μM) to obtain the near saturation of tubulin with the compound. Also, we have utilized the IKP-104-induced perturbations in the intrinsic fluorescence of tubulin itself at 330 nm (λ_{ex} = 273 nm) as a probe for IKP-104 binding to the tubulin molecule. As shown in Figure 1A, IKP-104 had an absorption maximum at 276 nm, very close to the absorption maximum

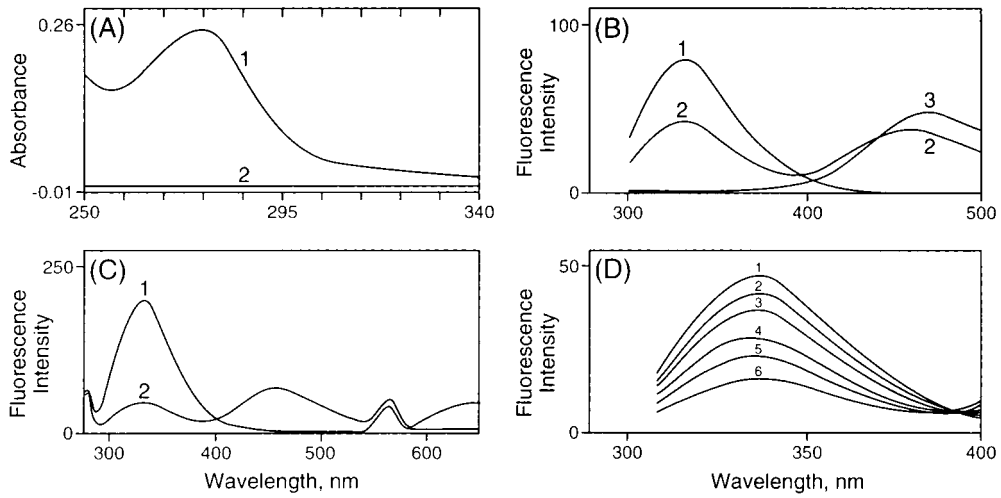

FIGURE 1: Spectral properties of IKP-104 binding to tubulin. (A) Absorption spectrum of 25 μM IKP-104 in 25% DMSO diluted in buffer (curve 1) and absorption spectrum of 25% DMSO in buffer (curve 2). (B) Fluorescence emission spectra (λ_{ex} = 273 nm) of unfractionated tubulin (2 μM) (curve 1), unfractionated tubulin (2 μM) in the presence of 25 μM IKP-104 (curve 2), and 25 μM IKP-104 alone (curve 3). (C) Emission spectra (λ_{ex} = 273 nm) of 2 μM $\alpha\beta_{IV}$ in the absence of IKP-104 (curve 1) and 2 μM $\alpha\beta_{IV}$ in the presence of 25 μM IKP-104 (curve 2). (D) Fluorescence emission spectra (λ_{ex} = 273 nm) of unfractionated tubulin (2 μM) in the presence of various concentrations of IKP-104: 0 μM (curve 1), 0.05 μM (curve 2), 0.2 μM (curve 3), 1.0 μM (curve 4), 10 μM (curve 5), and 25 μM (curve 6).

of tubulin, i.e., 273−276 nm. The components of the buffer, including DMSO, did not absorb significantly in the 260−340 nm range (Figure 1A). IKP-104 absorbed at 330 nm, but the absorbance of 25 μM IKP-104 at 330 nm (0.019) was approximately 7% of the absorbance at 276 nm (0.255). The unfractionated tubulin and IKP-104 exhibited emission maxima at 330 nm (mainly due to tryptophan residues) and 467 nm, respectively (Figure 1B). IKP-104 did not emit fluorescence at or near 330 nm; nor did unfractionated tubulin fluoresce at 467 nm. As shown in panels B and C of Figure 1, IKP-104 caused quenching of tryptophan fluorescence at 330 nm, presumably by altering the microenvironment of tryptophan residues via a conformational change. The extent of fluorescence quenching increased with increasing IKP-104 concentration (Figure 1D), and binding curves representing the near saturation of tubulin with the compound were obtained (Figure 2A−D). These curves are similar to near-saturation binding curves for IKP-104 reported in the literature (*4*, *7*−*9*). The data were analyzed using one-, two-, and three-site models. The Σq values (weighted sum of squares of the difference between the observed and calculated fluorescence intensities) were computed (Table 1) and subjected to the goodness-of-fit test. Irrespective of the type of tubulin that was used, the Σq values for the two-site model were substantially lower than those for the one-site model but the Σq values for the two-site model were either similar or substantially lower than the values for the three-site model (Table 1). Since this result favored the two-site model over the one- and three-site models, the results obtained using only the two-site model were considered. Analysis with the two-site model revealed that the IKP-104 binding curves (solid lines) for unfractionated tubulin (Figure 2A), $\alpha\beta_{II}$ (Figure 2B), and $\alpha\beta_{III}$ (Figure 2C) arise from the combination of two individual components (dotted lines) corresponding to the high- and low-affinity binding sites for the compound. In the case of $\alpha\beta_{IV}$, however, the binding curve resulted from only one component, apparently representing the high-affinity site; the component for the low-affinity site was absent (Figure 2D). The apparent dissociation constant for the high-affinity site (K_{d1}) on $\alpha\beta_{IV}$ was greater than those of unfractionated tubulin, $\alpha\beta_{II}$, or $\alpha\beta_{III}$. Both $\alpha\beta_{II}$ and $\alpha\beta_{III}$ had K_{d1} values that were lower than that of unfractionated tubulin (Table 1).

The observed differential affinities of tubulin isotypes for IKP-104 led us to measure the effect of IKP-104 on the polymerization of tubulin. At a low concentration (1.5 μM), the antitumor compound IKP-104 inhibited the tau-induced polymerization of unfractionated tubulin (Figure 3A) and isotypically pure $\alpha\beta_{II}$ (Figure 3B) and $\alpha\beta_{IV}$ (Figure 3D). The extent of inhibition varied among the isotypes. Interestingly, neither the extent nor the initial rate of tau-induced polymerization of $\alpha\beta_{III}$ (Figure 3C and Table 2) was affected significantly by 1.5 μM IKP-104. In general, the extent of tau-induced polymerization of isotypically pure tubulins appeared to be less sensitive to inhibition by 1.5 μM IKP-104 than that of unfractionated tubulin (Table 2). However, the effect of IKP-104 on the initial rate of polymerization of the unfractionated and isotypically pure tubulins was mixed. For example, unfractionated tubulin and $\alpha\beta_{IV}$ exhibited 48 and 70% loss in their rates of tau-induced polymerization, respectively, but in the case of $\alpha\beta_{II}$ and $\alpha\beta_{III}$ isotypes, IKP-104 did not seem to influence their rate of polymerization; in fact, a slight stimulation of the rate of polymerization of $\alpha\beta_{III}$ was observed (Table 2). The varied effect of IKP-104 on polymerization of different isotypes was also evident from the morphological differences among the polymers formed from different isotypes (Figure 4) in the presence of 1.5 μM IKP-104. Unfractionated tubulin and $\alpha\beta_{III}$ polymerized into microtubules and some aggregates. In contrast to $\alpha\beta_{III}$, $\alpha\beta_{II}$ polymerized into spirals. Surprisingly, $\alpha\beta_{IV}$ polymerized into microtubules without any trace of spirals or aggregates. These results raised the question of whether the microtubules formed from unfractionated and isotypically pure tubulins, in the absence of IKP-104 (Figure 4, lane 1), exhibit any differences among themselves in terms of the sensitivity toward low concentrations of IKP-104. As shown in Figure 4 (lane 3), 1.5 μM IKP-104 forced a large proportion of the preformed microtubules into aggregates

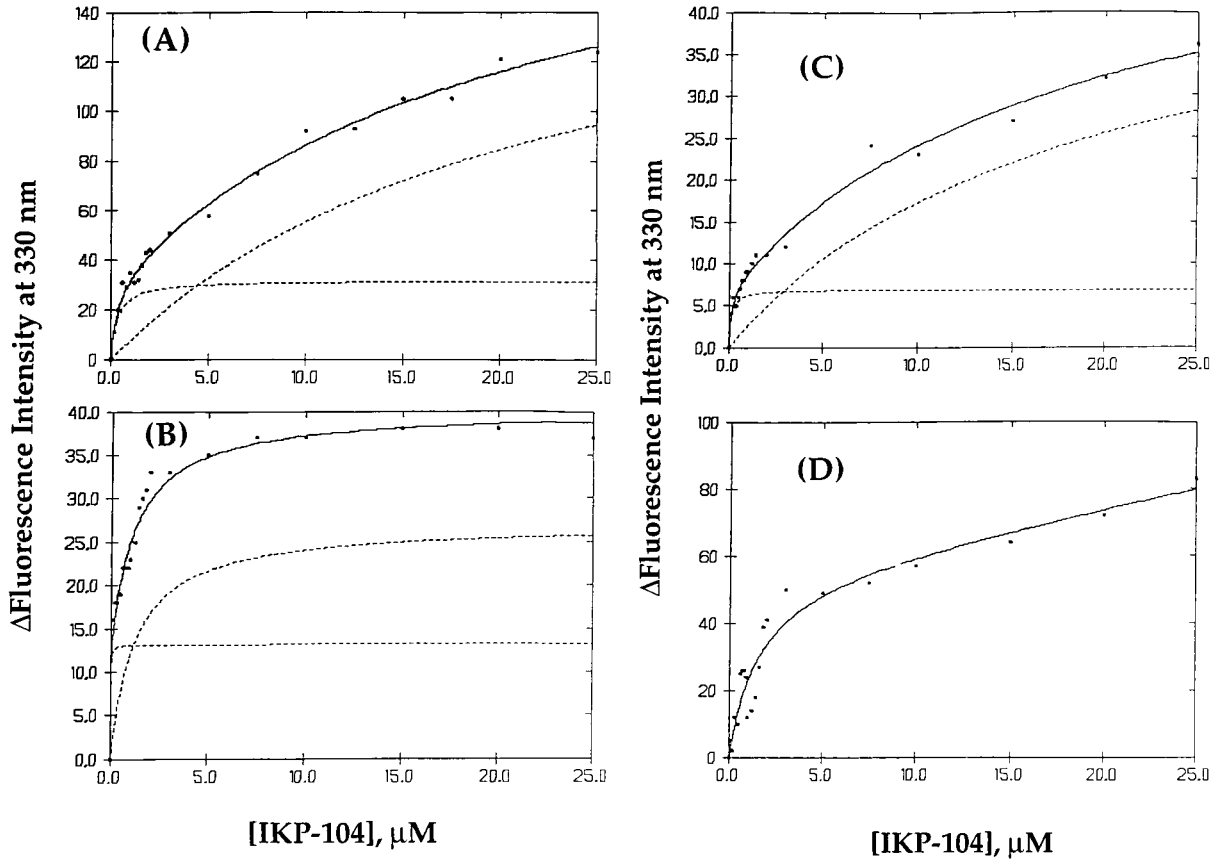

FIGURE 2: Binding of IKP-104 to unfractionated tubulin and to isotypically pure tubulins. Samples (500 μL) containing 2 μM tubulin and 0−25 μM IKP-104 were mixed at 4 °C, and then incubated at 30 °C for 30 min. The fluorescence of samples was measured at 330 nm by exciting the samples by 273 nm light. The differences in the fluorescence intensity of the tubulin−IKP-104 complex and IKP-104 (i.e., ΔF_{330} in arbitrary units) were plotted against IKP-104 concentrations, and the curves were analyzed as described in Experimental Procedures: (A) unfractionated tubulin, (B) $\alpha\beta_{II}$, (C) $\alpha\beta_{III}$, and (D) $\alpha\beta_{IV}$. The solid lines represent experimental curve, whereas the dotted lines represent hypothetical curves for high-affinity (lower curve) and low-affinity (upper curve) sites.

Table 1: Interaction of IKP-104 with Tubulin Isotypes

	Σq^a value				
tubulin	one IKP-104 binding site	two IKP-104 binding sites	three IKP-104 binding sites	$K_{d1}{}^b$ (μM)	$K_{d2}{}^b$ (μM)
unfractionated	1071	210	1072	0.32, 0.28	22, 14
$\alpha\beta_{II}$	171	48	48	0.007, 0.01	1.23, 1.18
$\alpha\beta_{III}$	199	24	60	0.11, 0.099	18, 16
$\alpha\beta_{IV}$	439	149	147	1.40, 1.88	*c*

[a] Σq values (sum of squares of the difference between the observed and calculated fluorescence intensities) were obtained by analysis of the data with one-, two-, and three-site models as described in Experimental Procedures. [b] The values of K_{d1} and K_{d2} were calculated from the data depicted in Figure 2 by using the equations for the two-site model, described in Experimental Procedures. The two values of K_{d1} and K_{d2} for each preparation of tubulin were obtained from two identical experiments. [c] Although the data for $\alpha\beta_{IV}$ were consistent with a two-site model, K_{d2} values deduced from the model were so high as to suggest very little binding to this site. An accurate measurement of this value would have required IKP-104 concentrations high enough to induce unfolding of the tubulin.

(unfractionated tubulin and $\alpha\beta_{III}$) and the spirals ($\alpha\beta_{II}$ isotype). However, this concentration of IKP-104 appeared to have no effect on the morphology of microtubules formed from $\alpha\beta_{IV}$; only microtubules were observed (Figure 4, lane 3, and Table 3).

The above differential effect of IKP-104 on microtubules was even more pronounced at higher concentrations. The absorbance of microtubules made from tau and tubulin, which did not change with time at steady state, was normalized to baseline followed by addition of 8 or 16 μM IKP-104 to the samples (Figure 5). Upon addition of IKP-104, an increase in the absorbance of samples in which tubulin was polymerized, presumably, into microtubules was observed (Figure 5). This increase in the absorbance was more prominent for unfractionated tubulin and $\alpha\beta_{IV}$ than for $\alpha\beta_{III}$ or $\alpha\beta_{II}$. Interestingly, $\alpha\beta_{IV}$ did not produce any spirals, whereas the unfractionated tubulin and both $\alpha\beta_{II}$ and $\alpha\beta_{III}$ produced microtubules as well as spirals (Figure 6 and Table 3). This would suggest that the IKP-104-induced increase in the absorbance of the samples containing microtubules is not due to depolymerization followed by aggregation or to the formation of the spirals because the $\alpha\beta_{IV}$ did not produce any spirals or aggregates but still exhibited a large increase in the absorbance in the presence of either 8 or 16 μM IKP-104. In the case of $\alpha\beta_{IV}$, the IKP-104-induced increase in the absorbance would suggest formation of aggregates or changes in morphology of pre-existing microtubules which were not large enough to be revealed under our electron microscopy experimental conditions.

As shown in Figure 6 and Table 3, unfractionated tubulin, $\alpha\beta_{II}$, and $\alpha\beta_{III}$ shared a common property, namely, the fact that microtubules formed from these tubulins in the presence of 1.5 μM IKP-104 were converted into spirals when the concentration of IKP-104 was increased from 1.5 to 8.5 μM.

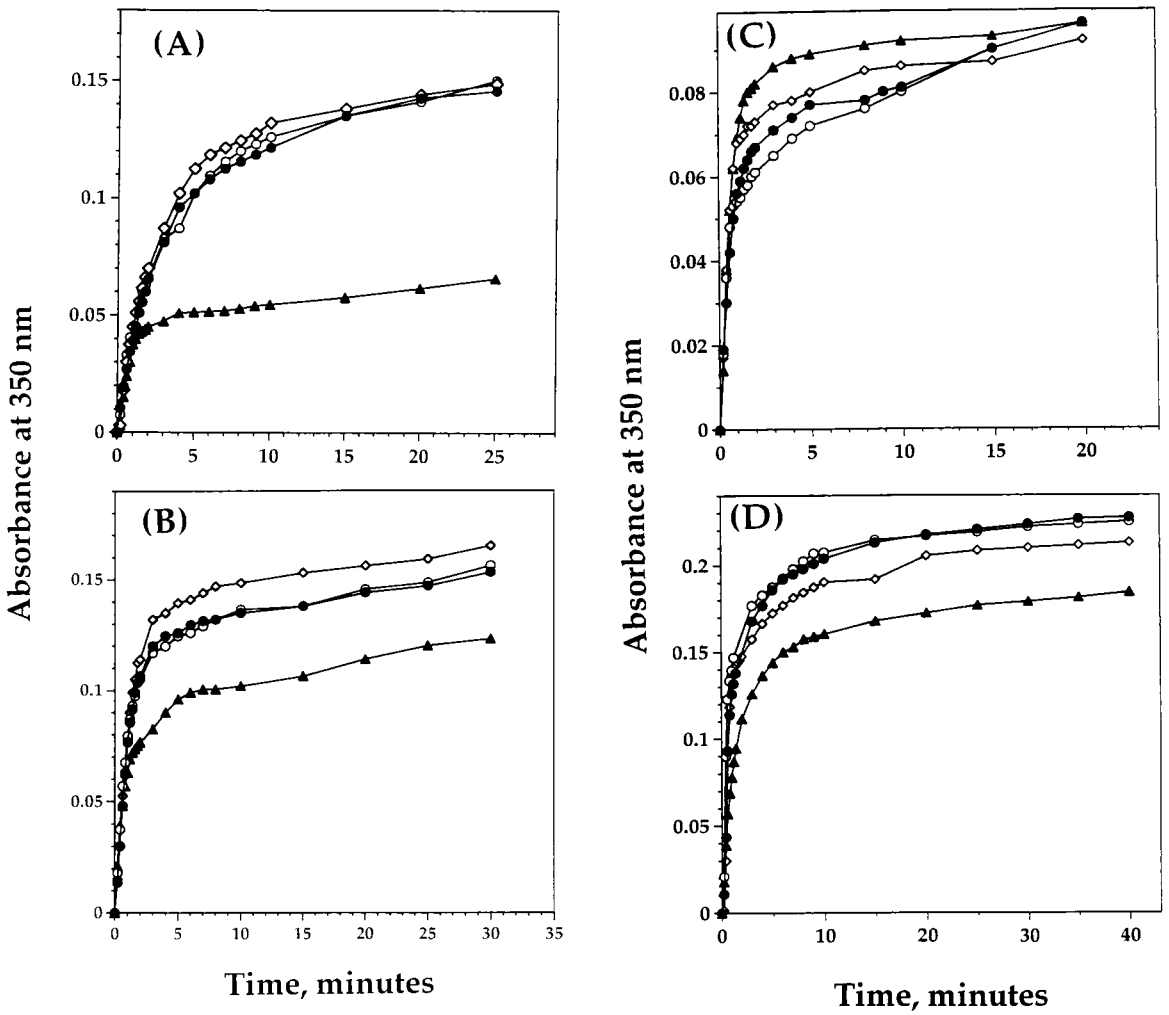

FIGURE 3: Effect of 1.5 μM IKP-104 on tau-induced polymerization of tubulin isotypes. Tubulin (1.5 mg/mL) was mixed with 0.15 mg/mL tau and either 1.5 μM IKP-104 or 0.7% DMSO. Polymerization was followed by turbidimetry as described in Experimental Procedures: (A) unfractionated tubulin, (B) $\alpha\beta_{II}$, (C) $\alpha\beta_{III}$, and (D) $\alpha\beta_{IV}$. In all the panels (A−D), symbols ●, ◇, and ○ represent incubation of 1.5 mg/mL tubulin and 0.15 mg/mL tau with 0.7% DMSO and the symbol ▲ represents incubation of 1.5 mg/mL tubulin and 0.15 mg/mL tau with 1.5 μM IKP-104.

Table 2: Effect of 1.5 μM IKP-104 on the Tau-Induced Assembly of Tubulin Isotypes[a]

tubulin	addition	extent [ΔA_{350} (nm)]	inhibition[b] (%)	rate[c] (ΔA_{350}/min)	inhibition[d] (%)
unfractionated	none	0.149	56	0.079	48
	IKP-104	0.066		0.041	
$\alpha\beta_{II}$	none	0.160	26	0.098	0
	IKP-104	0.119		0.098	
$\alpha\beta_{III}$	none	0.094	(2)	0.115	(3)
	IKP-104	0.096		0.119	
$\alpha\beta_{IV}$	none	0.221	17	0.360	70
	IKP-104	0.183		0.107	

[a] Aliquots (500 μL) of MES buffer containing 1.5 mg/mL tubulin and 0.15 mg/mL tau were incubated at 37 °C with or without 1.5 μM IKP-104, and microtubule assembly was followed at 350 nm. [b] After incubation for 40 min, ΔA_{350} values were used to calculate the % inhibition of assembly by assuming that the ΔA_{350} value for the samples incubated without IKP-104 was 100%. [c] The rate of the assembly was calculated from the maximum slope of the polymerization curves of tubulin in the presence and absence of IKP-104. [d] The % inhibition of the rate was calculated assuming that the rate of assembly of tubulin in the absence of IKP-104 was 100%. Numbers in parentheses represent an increase in the rate or extent of assembly.

$\alpha\beta_{IV}$ is an exception since it did not produce any significant number of spirals (Figure 6 and Table 3). This raises the possibility that although the microtubules formed in the presence or absence of low concentrations of IKP-104 may appear morphologically normal, addition of IKP-104 may introduce some subtle differences. This possibility was supported by a comparison of our data in Figures 4 and 6 which clearly demonstrated that in the case of $\alpha\beta_{IV}$, the microtubules formed in the absence of 1.5 μM IKP-104 were completely resistant to spiral formation when the IKP-104 concentration was increased to 8.5 μM.

IKP-104-induced formation of aggregates, spirals, and ribbon-like structures in the IKP-104-treated preparations of microtubules has been reported previously (*3*). Recently, the

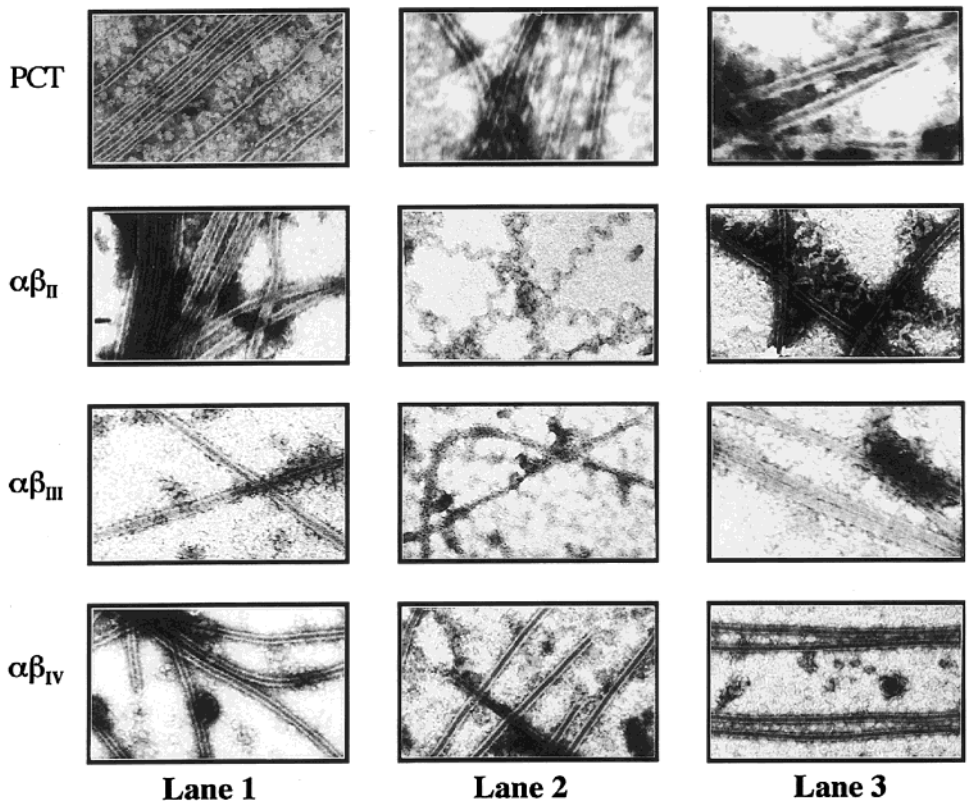

FIGURE 4: Effect of IKP-104 on the morphology of the microtubules. Three identical samples of assembly mixture containing 1.5 mg/mL tubulin and 0.15 mg/mL tau in MES buffer were placed on ice. Samples 1 and 3 contained 0.7% DMSO (lanes 1 and 3), and sample 2 contained 1.5 μM IKP-104 (lane 2). Assembly was initiated by warming the cuvettes to 37 °C. At steady state, 0.7% DMSO was added to samples 1 and 2 and 1.5 μM IKP-104 to sample 3, and the incubation was carried out for an additional 20 min. Thereafter, 50 μL aliquots were processed for electron microscopy. All the samples were analyzed at a magnification of 66 000 with the following exceptions: PCT, lane 2, 130 000 magnification; PCT, lane 3, 100 000 magnification; $\alpha\beta_{II}$, lane 2, 50 000 magnification; and $\alpha\beta_{IV}$, lane 3, 66 000 magnification.

Table 3: Effect of IKP-104 on the Morphology of Microtubules[a]

	preincubation			
	tubulin and tau in the absence of IKP-104			tubulin and tau in the presence of 1.5 μM IKP-104
tubulin	sample 1 1.5 μM IKP-104[b]	sample 2 8.5 μM IKP-104[b]	sample 3 17 μM IKP-104[b]	sample 4 8.5 μM IKP-104[b]
unfractionated	microtubules and some aggregates	microtubules and aggregates	microtubules, few spirals, and aggregates	all spirals
$\alpha\beta_{II}$	microtubules and few spirals	microtubules and spirals	mostly spirals and few microtubules	all spirals
$\alpha\beta_{III}$	microtubules and some aggregates	microtubules and spirals	microtubules and spirals	all spirals
$\alpha\beta_{IV}$	microtubules (no spirals)	microtubules (no spirals)	microtubules (no spirals)	microtubules and very few spirals

[a] Four identical samples of assembly mixture (350 μL) containing tubulin (1.0 mg/mL) and tau (0.1 mg/mL) were placed on ice. During preincubation, three of the samples did not contain any IKP-104 but did contain the compound solvent DMSO, while the fourth contained 1.5 μM IKP-104. Assembly was initiated by warming the cuvettes to 37 °C. At steady state, the IKP-104 concentration in samples 1−4 was raised to 1.5, 8.5, 17, and 8.5 μM, respectively. After incubation for approximately 20 min, samples were withdrawn for electron microscopy. The table describes the morphology of the tubulin polymers formed after the indicated treatments. [b] IKP-104 added at steady state to give this final concentration.

aggregation-induced decay of the unfractionated tubulin by IKP-104 has been related to the binding of the compound to the low-affinity site (*8*). Due to the absence of this site on $\alpha\beta_{IV}$, the polymers formed from $\alpha\beta_{IV}$ and tau in the presence of 1.5 μM IKP-104 comprised only microtubules but no spirals or ribbons (Figure 4). On the other hand, $\alpha\beta_{II}$, which had the strongest low-affinity site among the unfractionated tubulin and other isotypes, produced only spirals and ribbons and no microtubules (Table 1 and Figure 4). The polymers assembled from $\alpha\beta_{III}$ containing strong low-affinity sites consisted of both microtubules and aggregated material. It is also interesting to note that unfractionated tubulin, which is a complex mixture of several isotypes, including $\alpha\beta_{II}$, $\alpha\beta_{III}$, and $\alpha\beta_{IV}$, produced microtubules and aggregates, as well as spirals in the presence of 17 μM IKP-104 (Figure 6, lane 2).

DISCUSSION

In previous work aimed at investigating the effect of IKP-104 on microtubule assembly, Mizuhashi et al. (*3*) used whole microtubule protein which is a complex mixture of a number of tubulin isotypes and the microtubule-associated

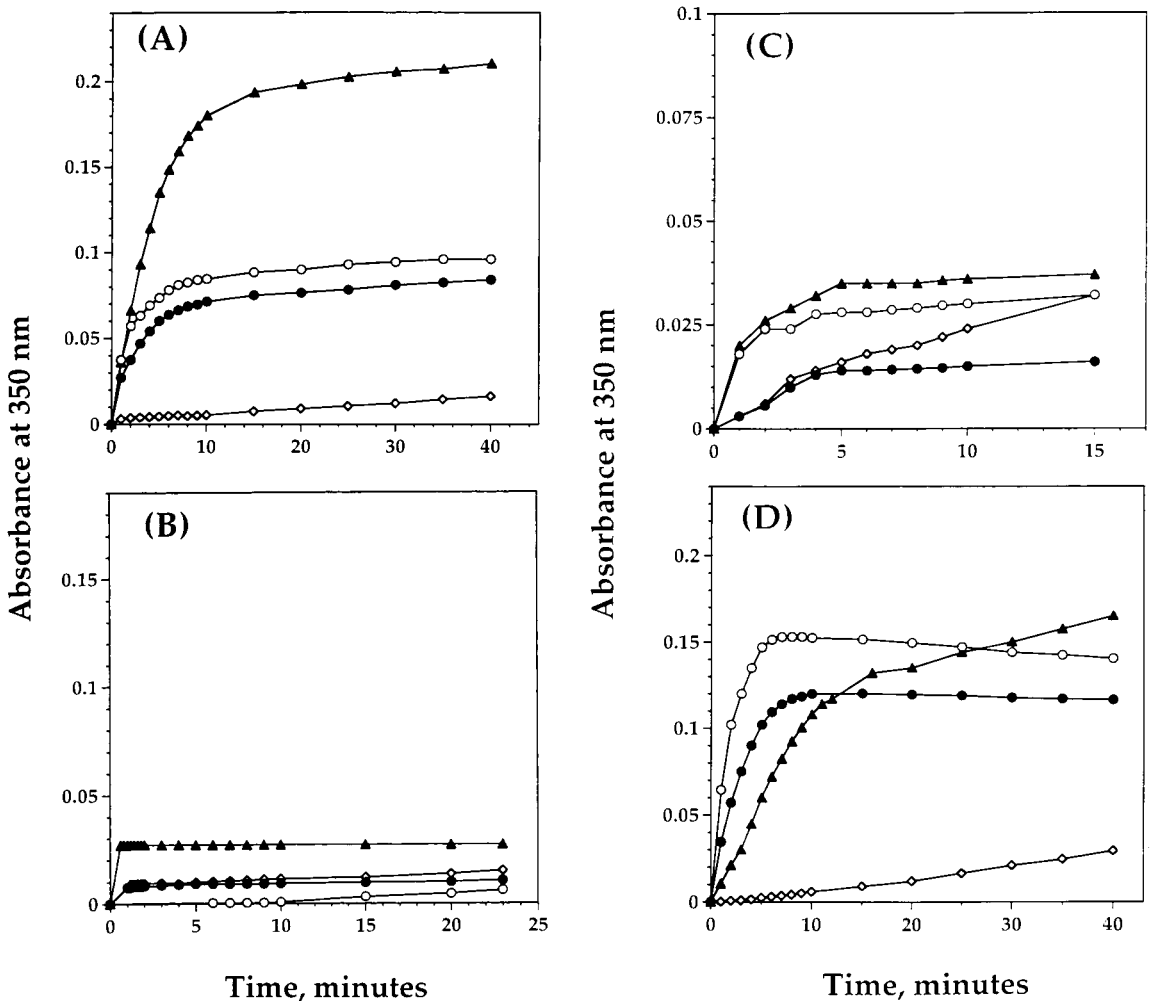

FIGURE 5: Effect of 8−16 μM IKP-104 on the microtubules formed from unfractionated tubulin and isotypically pure tubulin in the presence or absence of 1.5 μM IKP-104. The microtubules were formed from 1.5 mg/mL tubulin and 0.15 mg/mL tau in the presence of either 1.5 μM IKP-104 or 0.7% DMSO. After steady state had been achieved, the absorbance at 350 nm was adjusted to zero and the microtubules were incubated for an additional 40 min at 37 °C with the indicated amounts of IKP-104, and the change in the absorbance at 350 nm was recorded: (A) unfractionated tubulin, (B) $\alpha\beta_{II}$, (C) $\alpha\beta_{III}$, and (D) $\alpha\beta_{IV}$. Microtubules were formed from tubulin and tau in the absence of IKP-104; after steady state had been achieved, they were further incubated with either 1.5 (◇), 8 (●), or 16 μM IKP-104 (○). Microtubules were formed from tubulin and tau in the presence 1.5 μM IKP-104; after steady state had been achieved, they were further incubated with 8 μM IKP-104 (▲).

proteins (MAPs). In the work presented here, we have used tubulin which is not only pure but also fractionated into three dimers, differing in the nature of their β-subunits. Also, we have used only one form of MAP, i.e., tau, to polymerize microtubules. These considerations were based on the fact that the unfractionated tubulin which is used in most in vitro studies may not represent the composition of tubulin in vivo because relative tubulin isotype expression may be cell-specific (*19*). Moreover, the conclusions derived from the cellular, histochemical, and molecular studies on microtubules are converging to raise the possibility that each isotype of tubulin may have a unique conformation and function in the cell (*12*, *33*−*36*). Therefore, it is likely that individual isotypes of tubulin and thus microtubules formed from them will interact uniquely with IKP-104. As discussed below, we find that indeed this is the case.

The isotypically pure tubulins were found to be less sensitive to IKP-104 than the unfractionated tubulin. This would imply that the isotypic purity of tubulin confers a higher degree of structural stability on the molecule for resisting the destabilizing effect of IKP-104. However, this increase in stability varied from one isotype to another. Compared to that of $\alpha\beta_{II}$ and $\alpha\beta_{IV}$, the polymerization of $\alpha\beta_{III}$ was more resistant to IKP-104, suggesting a relatively more stable conformation for $\alpha\beta_{III}$. This conclusion is supported by a differential scanning calorimetry study in which the conformation of $\alpha\beta_{III}$ was found to be more rigid than that of $\alpha\beta_{II}$ (*20*). The conformation of $\alpha\beta_{IV}$ appeared to be even more unique when its binding to IKP-104 is compared with the binding of other isotypes. Like the unfractionated tubulin, the isotypically pure $\alpha\beta_{II}$ and $\alpha\beta_{III}$ tubulins possessed two classes of IKP-104 binding sites, one each of high and low affinity. In contrast to $\alpha\beta_{II}$ and $\alpha\beta_{III}$, $\alpha\beta_{IV}$ contained only a high-affinity site.

It has been proposed that IKP-104 confers additional stability on the tubulin molecule through its binding to the high-affinity site but destabilizes the tubulin molecule by binding to the low-affinity site (*4*, *7*, *8*). From the almost complete absence of the low-affinity site on $\alpha\beta_{IV}$ and the fact that it forms almost no spirals, it is very tempting to speculate that the low-affinity IKP-104 binding site on the tubulin molecule probably dictates the formation of the

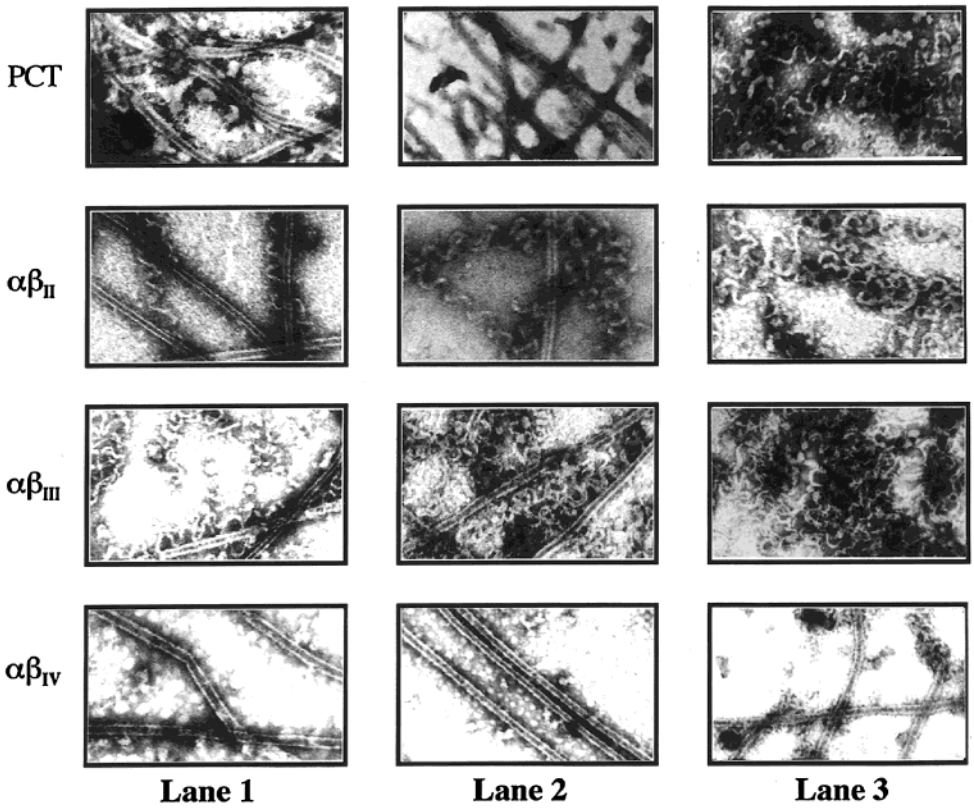

FIGURE 6: Effect of addition of IKP-104 on the morphology of the preformed microtubules. Three identical samples of the assembly mixture containing 1.5 mg/mL tubulin and 0.15 mg/mL tau were placed on ice. Two of them also contained 0.7% DMSO (lanes 1 and 2), while the third contained 1.5 μM IKP-104 (lane 3). Assembly was initiated by warming the cuvettes to 37 °C. At steady state, samples 1 and 3 received 8.5 μM IKP-104 (lanes 1 and 3), and sample 2 received 17 μM IKP-104 (lane 2). After incubation for approximately 20 min, 50 μL aliquots were processed for electron microscopy. All the samples were analyzed at a magnification of 66 000, except $\alpha\beta_{IV}$ in lane 1 (magnification of 100 000).

spirals or aggregates. Strong support for this speculation came from electron microscopy indicating generation of spirals by 1.5 μM IKP-104 in polymer preparations derived from $\alpha\beta_{II}$ tubulin which possesses the low-affinity site for the compound. However, the unfractionated tubulin and $\alpha\beta_{III}$, which possessed the low-affinity site for IKP-104, still did not produce the spirals in the presence of 1.5 μM IKP-104. It would not be unreasonable to assume that the low-affinity site on the tubulin should offer affinity of sufficient magnitude to IKP-104, to produce the spirals from tubulin. Thus, it is not surprising that unfractionated tubulin and the $\alpha\beta_{III}$ isotype having a low-affinity site almost 15−18-fold weaker than that of $\alpha\beta_{II}$ produced only a small amount of aggregates but not the spirals in the presence of 1.5 μM IKP-104.

The relationship between the high-affinity site for IKP-104 on tubulin and its effect on tubulin polymerization is complex. The presence of the dimers of tubulin, whether unfractionated or isotypically pure, in the polymerization mixture cannot be detected by turbidimetry, the method used for following the polymerization of tubulin. In turbidimetry, the increase in the absorbance at 350 nm during tau-induced polymerization of tubulin in the presence of IKP-104 could be due to the formation of microtubules, aggregates, spirals, or any combination of the three forms. For example, the unfractionated tubulin exhibited a 56% loss in the level of its tau-induced polymerization by 1.5 μM IKP-104 but still formed a large number of microtubules along with some aggregates. Also by turbidimetry, $\alpha\beta_{II}$ exhibited only 26% inhibition of its polymerization by 1.5 μM IKP-104 but did not form any microtubules. On the other hand, the polymerization of $\alpha\beta_{IV}$, as judged by turbidimetry, was affected more severely than that of $\alpha\beta_{II}$, but the polymerized form of $\alpha\beta_{IV}$ contained only the microtubules. From these results, it is proposed that in the case of the high-affinity-site also, it is the magnitude of the affinity which determines the overall effect of IKP-104 on the polymerization of tubulin and the morphology of the microtubules.

The proposal presented above is supported by our data which show that the high-affinity site on $\alpha\beta_{IV}$ (K_{d1} = 1.4 μM), which was the weakest among the isotypes and the unfractionated tubulin, made only a small population of $\alpha\beta_{IV}$ dimers incompetent for polymerization while the rest of the dimers polymerized into microtubules. On the other hand, the high-affinity site on $\alpha\beta_{II}$ (K_{d1} = 0.01 μM), being the strongest among the isotypes and the unfractionated tubulin, probably altered the tubulin conformation drastically by binding IKP-104 very tightly, the latter leading $\alpha\beta_{II}$ to its polymerization into the spirals but not microtubules.

The interaction of IKP-104 with the dimeric form of tubulin was slightly different from that in its polymeric form (microtubules). The most evident difference was observed in the case of $\alpha\beta_{II}$. In the presence of 1.5 μM IKP-104, the dimeric $\alpha\beta_{II}$ polymerized only into spirals. However, when microtubules were generated in the absence of IKP-104, subsequent addition of 1.5 μM IKP-104 caused only partial replacement of microtubules by spirals. Since the conformations of tubulin in its dimeric and polymeric states are

different (*37*, *38*), it is possible that the latter is relatively more resistant to IKP-104. The regions in the tubulin molecule affected by IKP-104 and the stoichiometries of tubulin and IKP-104, in dimeric and polymeric forms, are not yet known. Our electron microscopy data, however, suggest that the conformation of tubulin in the microtubules polymerized from the tubulin−IKP-104 complexes is relatively more labile than the conformation of tubulin in the microtubules polymerized from the tubulin in the absence of the compound. That is why the microtubules formed from unfractionated tubulin, $\alpha\beta_{II}$, and $\alpha\beta_{III}$ in the presence of low concentrations of IKP-104 were splayed into spirals by the addition of 8.5 μM IKP-104. But in the case of $\alpha\beta_{IV}$, the splaying of only very few microtubules into spirals by 8.5 μM IKP-104 was observed.

The interaction of tubulin isotypes with IKP-104 is clearly very complex, with a series of effects on assembly and the production of various morphologically distinct forms. It is possible that all the differences may arise from the differing affinities of the isotypes for IKP-104, but the possibility that roles are also played by the various post-translational modifications of tubulin (*39*−*42*) and the multiplicity of α-isotypes cannot be excluded.

ACKNOWLEDGMENT

We are thankful to Dr. Asok Banerjee for assistance in analysis of IKP-104 binding data and to Dr. Asish R. Chaudhuri for valuable discussions. We thank Veena Prasad, Mohua Banerjee, Patricia Schwarz, and Consuelo Walss for help during isolation of the microtubules from the bovine cerebra.

REFERENCES

1. Mizuhashi, F., Murata, K., Kitagaki, T., Nezu, M., Sano, M., and Tomita, I. (1990) *Jpn. J. Cancer Res. 81*, 1300−1306.
2. Mizuhashi, F., Murata, K., Kitagaki, T., and Tomita, I. (1991) *Jpn. J. Cancer Res. 82*, 1442−1447.
3. Mizuhashi, F., Murata, K., Kitagaki, T., and Tomita, I. (1992) *Jpn. J. Cancer Res. 83*, 211−218.
4. Ludueña, R. F., Roach, M. C., Prasad., Chaudhuri, A. R., Tomita, I., Mizuhashi, F., and Murata, K. (1995) *Biochemistry 34*, 15751−15759.
5. Hyams, J. S., and Lloyd, C. W. (1995) *Microtubules*, Wiley-Liss, New York.
6. Prasad, V., Chaudhuri, A. R., Curcio, M., Tomita, I., Mizuhashi, F., Murata, K., and Ludueña, R. F. (1998) *J. Protein Chem. 17*, 663−668.
7. Chaudhuri, A. R., Tomita, I., Mizuhashi, F., Murata, K., and Ludueña, R. F. (1998*) J. Protein Chem. 17*, 685−690.
8. Chaudhuri, A. R., Tomita, I., Mizuhashi, F., Murata, K., and Ludueña, R. F. (1998*) J. Protein Chem. 17*, 303−309.
9. Chaudhuri, A. R., Tomita, I., Mizuhashi, F., Murata, K., Potenziano, J. L., and Ludueña, R. F. (1998) *Biochemistry 37*, 17157−17162.
10. Avila, J. (1997) *Cancer J. 10*, 315−318.
11. Little, M., and Seehaus, T. (1988) *Comp. Biochem. Physiol. 90B*, 655−670.
12. Ludueña, R. F. (1998) *Int. Rev. Cytol. 178*, 207−275.
13. Lopata, M. A., and Cleveland, D. W. (1987) *J. Cell Biol. 105*, 1707−1720.
14. Hoyle, H. D., and Raff, E. C. (1990) *J. Cell Biol. 11*, 1009−1026.
15. Banerjee, A., Roach, M. C., Trcka, P., and Ludueña, R. F. (1992) *J. Biol. Chem. 267*, 5625−5630.
16. Renthal, R., Schneider, B. G., Miller, M. M., and Ludueña, R. F. (1993) *Cell Motil. Cytoskeleton 25*, 19−29.
17. Panda, D., Miller, H. P., Banerjee, A., Ludueña, R. F., and Wilson, L. (1994) *Proc. Natl. Acad. Sci. U.S.A. 91*, 11358−11362.
18. Sharma, J. S., and Ludueña, R. F. (1994) *J. Protein Chem. 13*, 165−175.
19. Roach, M. C., Boucher, V. L., Walss, C., Ravdin, P. M., and Ludueña, R. F. (1998*) Cell Motil. Cytoskeleton 39*, 273−285.
20. Schwarz, P. M., Liggins, J. R., and Ludueña, R. F. (1998) *Biochemistry 37*, 4687−4692.
21. Banerjee, A., and Ludueña, R. F. (1992) *J. Biol. Chem. 267*, 13335−13339.
22. Derry, W. B., Wilson, L., Khan, I. A., Ludueña, R. F., and Jordan, M. A. (1997) *Biochemistry 36*, 3554−3562.
23. Khan, I. A., and Ludueña, R. F. (1994) *Mol. Biol. Cell 5*, 284a.
24. Khan, I. A., and Ludueña, R. F. (1995) *Mol. Biol. Cell 6*, 30a.
25. Fellous, A., Francon, J., Lennon, A. M., and Nunez, J. (1977) *Eur. J. Biochem. 78*, 167−174.
26. Khan, I. A., and Ludueña, R. F. (1996) *Biochemistry 35*, 3704−3711.
27. Laemmli, U. K. (1970) *Nature 227*, 680−685.
28. Crestfield, A. M., Moore, S., and Stein, W. H. (1963) *J. Biol. Chem. 238*, 622−627.
29. Ludueña, R. F., Roach, M. C., Trcka, P. P., Little, M., Palanivalu, P., Binkley, P., and Prasad, V. (1982) *Biochemistry 21*, 4787−4794.
30. Banerjee, A., Roach, M. C., Trcka, P., and Ludueña, R. F. (1990) *J. Biol. Chem. 265*, 1794−1799.
31. Lowry, O. H., Rosebrough, N. J., and Randall, R. J. (1951) *J. Biol. Chem. 193*, 265−275.
32. Lakowicz, J. R. (1983) *Principles of Fluorescence Spectroscopy*, pp 1−44, Plenum Press, New York.
33. Ranganathan, S., Salazar, H., Benetatos, C. A., and Hudes, G. R. (1997) *Prostate 30*, 263−268.
34. Lu, Q., Moore, G. D., Walss, C., and Luduena, R. F. (1998) *Adv. Struct. Biol. 5*, 203−227.
35. Armas-Portela, R., Parrales, M. A., Albar, J. P., Martinez, A. C., and Avila, J. (1999) *Exp. Cell Res. 248*, 372−380.
36. Walss, C., Kreisberg, J. I., and Ludueña, R. F. (1999) *Cell Motil. Cytoskeleton 42*, 274−284.
37. Kotani, S., Kawai, G., Yokoyama, S., and Murofushi, H. (1990) *Biochemistry 29*, 10049−10054.
38. Audenaert, A., Heremans, L., Heremans, K., and Engelborghs, Y. (1989) *Biochim. Biophys. Acta 996*, 110−115.
39. MacRae, T. H. (1997) *Eur. J. Biochem. 244*, 265−278.
40. Redeker, V., Rossier, J., and Frankfurter, A. (1998) *Biochemistry 37*, 14838−14844.
41. Regnard, C., Audebert, S., Desbruyeres, D. P., and Eddé, B. (1998) *Biochemistry 37*, 8395−8404.
42. Schneider, A., Plessmann, U., Felleisen, R., and Weber, K. (1999) *Parasitol Res. 85*, 246−248.

BI000331O